Review

Interventional Cardiology

Noninvasive hemodynamic assessment using coronary computed tomography angiography: the present and future

Jun-Bean Park[1] & Bon-Kwon Koo*[,1]

[1]Department of Medicine, Seoul National University Hospital, Seoul, 110–744, South Korea

*Author for correspondence:
Tel.: + 82 2 2072 2062
Fax: +82 2 3675 0805
bkkoo@snu.ac.kr

The paradigm has been shifted from anatomy-guided to physiology-guided management of coronary artery disease. Hence, intense attention has been focused on whether hemodynamic assessment can be achieved by noninvasive imaging modalities. Among them, coronary computed tomography (CT) has potentials to allow the assessment of ischemia-causing coronary stenosis due to its excellent spatial resolution. Currently, myocardial perfusion imaging, CT-derived computed fractional flow reserve and transluminal attenuation gradient are promising CT-based techniques to detect myocardial ischemia. Furthermore, its application can be extended beyond the detection of ischemia and to the measurement of hemodynamic forces acting on the plaque and the simulation of treatment plans using virtual stenting technique.

Keywords: coronary artery disease • coronary computed tomography angiography • fractional flow reserve • hemodynamics • myocardial perfusion imaging • noninvasive diagnostic method • transluminal attenuation gradient

Clinical relevance of hemodynamic assessment in patients with coronary artery disease (CAD) has been increasingly recognized, with special focus on its ability to identify the clinically significant ischemia-causing lesion. For example, fractional flow reserve (FFR), the ratio of maximal blood flow in a stenotic artery to the normal maximal flow can provide valuable information for the diagnosis of functionally significant stenosis [1]. More importantly, FFR-based treatment strategy can improve the clinical outcomes in CAD patients, compared with those with angiography-guided intervention [2] or with medical therapy [3]. All these findings fortify the importance of myocardial ischemia in predicting the future risk of cardiovascular events. Thus, current guidelines strongly recommend the clinical use of FFR to guide coronary revascularization [4,5,6]. However, like coronary angiography, the inevitably invasive nature of FFR hampers its wide applicability, underscoring the need of novel technique for accurate and noninvasive assessment of myocardial ischemia.

Traditional noninvasive imaging modalities, however, such as single-photon emission CT (SPECT), has been suffering from relatively high false-negative rate to detect myocardial ischemia in patients with left main or multivessel disease due to the low spatial resolution and balanced ischemia. As compared with other imaging methods, computed tomography (CT) has the potential to overcome these limitations due to its submillimeter spatial resolution and excellent image quality. Indeed, the advances in CT imaging technology enable to image the entire coronary arterial trees and to provide anatomical information on the coronary lumen and wall. Furthermore, currently available coronary CT angiography (cCTA) can detect the transmural difference in myocardial perfusion, translating into the presence of ischemia or infarct. More importantly, computational fluid dynamics (CFD) technology makes it possible to simulate coronary flow conditions in a patient-specific coronary model and noninvasive assessment of *in vivo* hemodynamic parameters, such as pressure and FFR [7,8,9,10,11]. These improvements

Future Medicine

not only minimize the major limitation of cCTA, the low specificity and positive predictive value for significant CAD, but also enable cCTA can be used as a 'one-stop shop' for the management of CAD patients. During recent years, mounting evidence has been provided that the CT-based functional imaging becomes a feasible and accurate method to identify the ischemia-causing stenosis. Furthermore, some exploratory studies have illustrated the potential role of CT-based hemodynamic assessments which can be applicable in the diagnosis and treatment planning of CAD.

The present status of cCTA-based hemodynamic assessment

Currently, the clinical usefulness of cCTA-based hemodynamic assessment has been evaluated primarily for the detection of myocardial ischemia. Many studies have already proved that several different techniques based on cCTA, particularly CT-myocardial perfusion imaging (MPI), CT-derived FFR and transluminal attenuation gradient (TAG) by CT, can provide the information on the presence of myocardial ischemia in CAD patients (Table 1).

Computed tomography-myocardial perfusion imaging

One way of CT-based hemodynamic assessment is to examine the degree of myocardial perfusion (Figures 1 & 2). Stress CT-myocardial perfusion imaging (CT-MPI) is a novel examination technique that provides both anatomic and functional information (i.e., the presence of myocardial ischemia) [17]. In general, the protocol of CT-MPI is composed of image acquisitions at rest and stress phases, similar to a conventional nuclear MPI study. Both in rest and stress acquisitions, iodinated contrast agent is administered (60–75 ml for each acquisition) for a total dose of approximately 130–150 ml. Using the rest acquisition, this technique provides myocardial perfusion information during resting condition as well as coronary anatomy. Imaging acquisition of stress phase is performed under pharmacological stress conditions by administering adenosine, regadenoson or dipyridamole, which is similar to nuclear MPI exam [17]. To determine the presence of perfusion defect, two imaging criteria are generally used. The first criterion is a low-density lesion conforming to the coronary territory, and the second one is the persistence of the lesion throughout the cardiac cycle as seen on the cine image. The presence and extent of the myocardial perfusion defect is assessed using multiphase cardiac images according to the AHA 16-segment model. Review of the multiphase images is often helpful to differentiate the true perfusion defect from the artifact. For example, the low density area of the myocardium disappeared during a different cardiac phase in the case of a motion artifact.

Table 1. Summary of published clinical trials evaluating the diagnostic performance of computed tomography-myocardial perfusion imaging, fractional flow reserve from coronary computed tomography angiography data and transluminal attenuation gradient.

Techniques	Author (year)	Scanner	Comparison	N	Sn (%)	Sp (%)	PPV (%)	NPV (%)	Ref.
CT-MPI	Blankstein *et al.* (2009)	DSCT	CT-MPI and SPECT vs QCA	33	92	67	89	75	[12]
CT-MPI	George *et al.* (2009)	64/256-MDCT	cCTA/CT-MPI vs QCA/SPECT	27	86	92	92	85	[13]
CT-MPI	Ho *et al.* (2010)	Second-generation DSCT	Dynamic CT-MPI vs SPECT/QCA	35	95	65	78	79	[14]
FFR_{CT}	Koo *et al.* (2011)	64- or higher MDCT	FFR_{CT} vs invasive FFR (per vessel basis)	103	88	82	74	92	[9]
FFR_{CT}	Min *et al.* (2012)	64- or higher MDCT	FFR_{CT} vs invasive FFR (per patient basis)	252	90	54	67	84	[10]
FFR_{CT}	NØrgaard *et al.* (2014)	64- or higher MDCT	FFR_{CT} vs invasive FFR (per patient basis)	254	86	79	65	93	[11]
TAG	Choi *et al.* (2011)	64-MDCT	TAG vs QCA	126	93	69	85	83	[15]
TAG	Yoon *et al.* (2012)	64-MDCT	TAG vs invasive FFR (per vessel basis)	53	38%	88%	67%	69%	[16]

cCTA: Coronary computed tomography angiography; CT-MPI: Computed tomography-myocardial perfusionimaging; CT: Computed tomography; DSCT: Dual source computed tomography; FFR: Fractional flow reserve; FFR_{CT}: computed tomography-derived fractional flow reserve; MDCT: Multi-detector computed tomography; N: Number; NPV: Negative predictive value; PPV: Positive predictive value; QCA: Quantitative coronary angiography; Sn: Sensitivity; Sp: Specificity; SPECT: Single-photon emission computed tomography; TAG: Transluminal attenuation gradient.

A previous study using canine model has shown that the adenosine-augmented CT-MPI is a feasible diagnostic tool to detect perfusion deficits, which was validated against microsphere-derived myocardial blood flow as a reference standard [18]. Several clinical studies have also supported the utility of MPI, by demonstrating high diagnostic accuracy in comparison with traditional myocardial perfusion imaging tests [12,13,19,20]. Specifically, Blankstein *et al.*, reported that the diagnostic accuracy of CT-MPI to detect stenosis ≥50% was favorably comparable to that of SPECT on the per-vessel basis (sensitivity 79 vs 67% and specificity 80 vs 83%) and even identical on the per-patient basis (sensitivity 92 vs 92% and specificity 67 vs 67%). When compared with invasively measured FFR, Ko *et al.*, demonstrated that the combination of CT-MPI with cCTA can be accurate to identity hemodynamically significant stenoses in patients with suspected CAD (accuracy 92%, sensitivity 87% and specificity 95%) [20]. Given the high accuracy of cCTA for the morphological evaluation of CAD, the ability to simultaneously visualize both anatomic coronary stenosis and physiologic consequences is an important advantage from a clinical perspective.

Several studies have demonstrated that the identification of myocardial perfusion deficits at rest and pharmacological stress is feasible by employing two different approaches: 'single-phase CT acquisitions' and 'dynamic CT acquisitions.' The first approach relies on a single CT acquisition at rest or adenosine-induced stress condition after injection of a contrast agent [21]. The most significant advantage of this approach is a relatively low level of radiation exposure. A previous study has shown that a comprehensive work-up based on single-phase acquisitions can be performed with radiation doses similar to myocardial SPECT of approximately 12 mSv [12]. Furthermore, with introduction of high-pitch imaging, radiation doses can be reduced below 3 mSv [21]. However, this approach is based on mere comparisons of enhancement between apparently poststenotic versus normal myocardial segments (single-phase enhancement), the assessment of myocardial perfusion is limited to a qualitative or semiquantitative analysis. The latter approach, by using sequential CT acquisitions, enables dynamic imaging of contrast agent kinetics and generation of time-attenuation curves, and thus permits a truly quantitative assessment of myocardial blood flow at rest and stress conditions [14,22]. There is early evidence that the quantification of myocardial blood flow by adenosine-stress CT-MPI is well correlated with coronary artery blood flow and FFR, which is the experimental and clinical reference standard, respectively [23]. As a tradeoff, however, this approach is related to higher radiation exposure. Fortunately, it has been suggested that radiation exposure can be substantially reduced without loss of image quality by future optimization and the adaptation of iterative reconstruction technique [24].

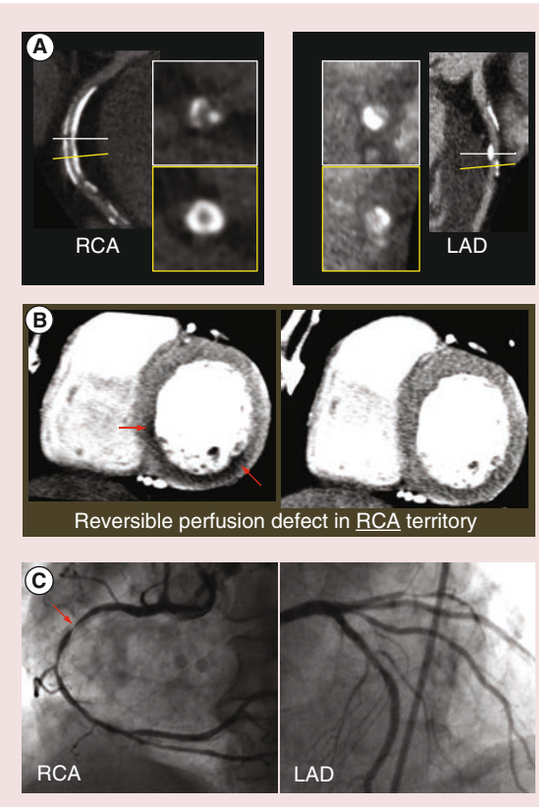

Figure 1. Example of comprehensive assessment of anatomic stenosis and hemodynamic significance using static computed tomography;-myocardial perfusion imaging. (A) When heavily calcified plaques are present, it is difficult to clearly assess the degree of luminal narrowing by cCTA. The blooming artifact resulted from calcified plaques is one of major limitations of cCTA. **(B)** A reversible perfusion defect (red arrows) is detected in inferior and inferoseptal walls which is RCA territory. **(C)** On invasive coronary angiography, tight stenosis in RCA (red arrows) is confirmed whereas there is no significant stenosis in LAD.
cCTA: Coronary computed tomography; angiography; LAD: Left anterior descending coronary artery; RCA: Right coronary artery.

As shown in Table 2, CT-MPI has several strengths compared with other CT-based functional imaging. First, CT-MPI can provide direct visualization of myocardium with and without perfusion deficits. This advantage can be particularly helpful in the setting of stenosis and is difficult to evaluate, such as calcified coronary arteries. Second, CT-MPI can be easily performed with no need for special software. However, this imaging method also has a number of limitations. First, there are concerns regarding additional radia-

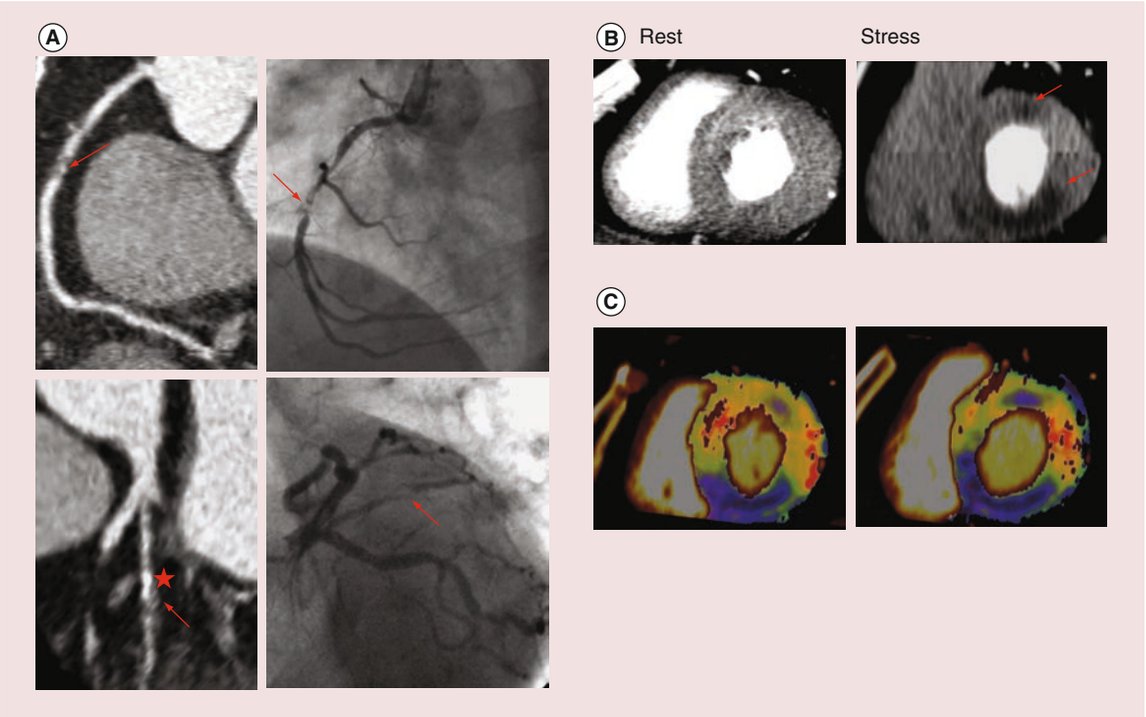

Figure 2. Example of comprehensive assessment of anatomic stenosis and hemodynamic significance using dynamic computed tomography-myocardial perfusion imaging. (A) Reconstructed cCTA images and invasive coronary angiography showing stenotic lesions (red arrows) of RCA and RI. Note that the presence of heavy calcification (red asterisk) hampers accurate measures of stenosis severity in the RI lesion, whereas cCTA clearly visualize the near total occlusion of mid RCA. **(B)** Rest and stress CT-MPI depicting reversible myocardial perfusion defects in territories of RCA and RI (red arrows). Perfusion defects are presented in RI territory as well as RCA territory, suggesting both stenoses are flow-liming. Note that a prominent misregistration artifact on the stress image. This artifact can be developed by the integration of images in different cardiac phases, if two image acquisitions are required to perform dynamic CT-MPI. Thus, the misregistration artifact is not found on static CT-MPI images, and it can also be avoided with a dynamic scanner capable of covering the entire heart by a single image acquisition. **(C)** Quantitative color map representing the distribution of myocardial blood flow. Blue color of RCA and RI territories indicates the reduction of myocardial blood flow in these coronary territories.
cCTA: Coronary CT angiography; CT: Computed tomography; CT-MPI: Computed tomography-myocardial perfusion imaging; RCA: Right coronary artery; RI: Ramus intermedius.
Images were provided by Dong Hyun Yang from Asan Medical Center, South Korea.

tion exposure as CT-MPI requires two scans with rest and stress conditions. Second, adenosine should be used to induce maximal hyperemia for CT-MPI at present, which has a risk causing discomfort or other adverse events to patients. Various efforts have been made to solve this issue, and other vasodilator agents have gained attention as alternatives to adenosine, For example, regadenoson, a selective A2A adenosine receptor agonist, has been reported to provide comparable diagnostic performance and better tolerance than adenosine [17,25,26]. Third, there are several artifacts that should be kept in mind when performing and interpreting CT-MPI, namely, motion artifact and beam hardening [17]. Motion artifact is a significant source of misinterpretation, since cardiac motion during image acquisitions leads to hypoenhanced regions which can mimic true perfusion defects. Fortunately, as the temporal resolution of CT continues to improve, motion artifact will be less of an issue in the future. Beam hardening is a phenomenon which occurs when the x-ray beam passes through a high density object. Because this phenomenon leads to a selective attenuation of lower-energy beams and increased mean energy of remaining beams, hypoenhanced areas can be found as an artifact that can mimic regions of true perfusion defect. Attempts to develop an algorithm to minimize this artifact are ongoing.

Computed tomography-derived fractional flow reserve

At present, FFR is the gold standard invasive method for the identification of stenotic lesions which cause myocardial ischemia [30]. This pressure-derived flow index represents the ratio of coronary flow distal to a coronary stenosis to normal maximal coronary blood flow. However, measurement of FFR requires

invasive cardiac catheterization, intravenous or intracoronary adenosine administration and an expensive coronary pressure wire. Because CFD is a branch of fluid mechanics to solve the problems involving physical fluid flows with the use of numerical methods and computational algorithms, many attempts have been made to apply CFD to analyze blood flow in vascular systems. Recent studies have reported that CFD models reconstructed from routinely obtained CT images can be used to demonstrate the hemodynamic conditions and changes in various vascular beds, including intracranial arteries and aorta [31,32]. Advances in CFD can also make it possible to simulate coronary blood flow, velocity of blood and pressure-related metrics on the patient-specific coronary tree [7]. Maximal hyperemic coronary flow can also be simulated, which occurs with adenosine infusion for the measurement of invasive FFR. The application of CFD on standard cCTA images allows the calculation of FFR from cCTA data (FFR_{CT}) (Figure 3) [8,33]. In general, computation of FFR_{CT} requires the combination of three key components: construction of an anatomic model of the coronary arterial tree, a mathematical model of coronary physiology to derive boundary conditions and a numerical solution of the laws of physics governing fluid dynamics [8]. FFR_{CT} technique is now commercially available in several countries. The three key principles of FFR_{CT} are as follows: the total resting coronary flow is estimated based on the myocardial mass, by assuming that coronary supply meets myocardial demand at rest, resistance of the microcirculation at rest is inversely but not linearly proportional to the size of the feeding vessel and microcirculation reacts predictably to the maximal hyperemia in subjects with normal coronary blood flow. Based on these principles, a lumped parameter model representing the resistance to flow during simulated maximal hyperemic conditions is applied to each coronary arterial branch of the cCTA model, and the FFR_{CT} is computed for the entire coronary tree.

Several studies assessed the diagnostic performance of FFR_{CT} by comparing to that of the reference standard invasive FFR or cCTA alone [9,10,11]. First, investigators in the Diagnosis of Ischemia-Causing Stenoses Obtained Via Noninvasive Fractional Flow Reserve (DISCOVER-FLOW) trial compared diagnostic performance of FFR_{CT} with that of percent diameter stenosis from cCTA, and showed the improved per-vessel diagnostic accuracy (84.3 vs 58.5%) which was mainly derived from increased specificity (82.2 vs 39.6%) with no substantial loss of sensitivity (87.9 vs 91.4%) [9]. In this study, FFR_{CT} had larger area under the receiver-operator characteristics curve (AUC) in identifying ischemia-causing lesions than cCTA (0.90 vs 0.75, p = 0.001). Second, the Determination of Fractional Flow Reserve by Anatomic Computed Tomographic Angiography (DeFACTO) trial demonstrated that FFR_{CT} had superior per-patient diagnostic performance to cCTA alone with respect to the identification of ischemic lesions (accuracy 73 vs 64%, sensitivity 90 vs 84% and specificity 54 vs 42%) [10]. The discrimination power to determine ischemia-causing lesions was

Table 2. Strength and limitation of computed tomography-myocardial perfusion imaging, fractional flow reserve from coronary computed tomography angiography data and transluminal attenuation gradient.

	Key concept	Pros	Cons	Ref.
CT- MPI	Assessment of myocardial ischemia by detecting the low density area of the myocardium	Direct view of myocardium	Requirement of adenosine	[17,27]
		No special software	Radiation dose concern (two scans)	
		Easy to perform	Artifacts affecting interpretation	
FFR_{CT}	Assessment of lesion-specific ischemia by computing FFR from CFD methods applied to cCTA data	Precise detection of ischemia-causing lesion	Indirect view of ischemia	[8,28]
		No requirement of adenosine	No information on perfusion	
		No additional scan	Need supercomputer	
TAG	Assessment of ischemia-causing stenosis by measuring gradient of intraluminal radiological attenuation across lesion	No additional radiation or contrast	Artifacts affecting interpretation	[29]
		No requirement of off-site computation	Relatively limited data	

cCTA: Coronary computed tomography angiography; CFD: Computational fluid dynamics; CT: Computed tomography; CT-MPI: Computed tomography-myocardial perfusion imaging; FFR: Fractional flow reserve; FFR_{CT}: Computed tomography-derived fractional flow reserve; TAG: Transluminal attenuation gradient.

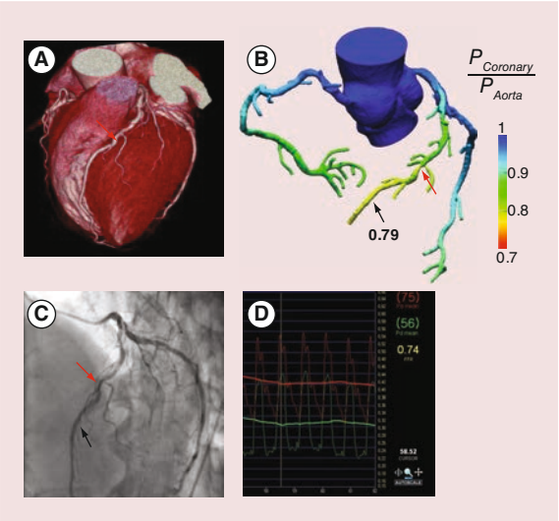

Figure 3. A representative case of computed tomography-derived fractional flow reserve. (A) Conventional cCTA detects a focal luminal narrowing (red arrow) in the distal LAD. **(B)** The FFR_{CT} demonstrates that the aforementioned focal stenosis (red arrow) is responsible for ischemia, with a computed value of 0.76 (black arrow). **(C)** Invasive coronary angiography confirms the stenotic segment in LAD (red arrow), and invasive FFR is measured at the corresponding point where FFR_{CT} is calculated (black arrow). **(D)** The value of invasive FFR is 0.74, which is similar to that of FFR_{CT}.
cCTA: Coronary computed tomography angiography; CT:Computed tomography; FFR: Fractional flow reserve; FFR_{CT}: Computed tomography-derived fractional flow reserve; LAD: Left anterior descending coronary artery.

also better for FFR_{CT} than cCTA alone (AUC 0.81 vs 0.68, p <0.001). Third, the Analysis of Coronary Blood Flow Using CT Angiography: Next Steps (NXT) trial recently reported that FFR_{CT} can offer comparable per-patient diagnostic accuracy to invasive FFR measurement for the diagnosis of hemodynamically significant lesions in patients with suspected stable CAD (accuracy 81 vs 77%, sensitivity 86 vs 64% and specificity 79 vs 83%) [11]. When compared with cCTA, FFT_{CT} provided markedly improved specificity without compromising the acceptable level of sensitivity (accuracy 81 vs 53%, sensitivity 86 vs 94% and specificity 79 vs 34%), leading to the larger AUC for the detection of myocardial ischemia (0.90 vs 0.81, p value = 0.0008). Of note, the diagnostic accuracy of FFR_{CT} remained high in patients with intermediate stenosis (accuracy 80%, sensitivity 85% and specificity 79%).

This state-of-the-art FFR_{CT}-based hemodynamic assessment has several strengths over other methods (Table 2). Most importantly, FFR_{CT} permits the precise identification of lesions responsible for myocardial ischemia. In this regard, FFR_{CT} may yield the improvement in test specificity to detect hemodynamically significant lesions, compared with previous other stress imaging tools. Furthermore, this ability to pinpoint the culprit lesion for ischemia can be helpful in planning the treatment strategy. On the other hand, FFR_{CT} has also some limitations to be considered. First, because the computation of FFR_{CT} requires accurate anatomic models of coronary arteries, various artifacts such as motion, calcification and misregistration may limit the accuracy of FFR_{CT}. Thus, it is essential to strictly adhere to the protocols ensuring good quality of data and facilitating accurate lumen boundary descriptions. Second, since major assumptions in the physiological models are based on population-specific as well as patient-specific data, these assumptions may be incorrect in patients with certain conditions. For example, considering that physiologic functions to reduce the resistance in response to adenosine-mediated hyperemia is impaired in patients with microvascular disease, the degree of vasodilation can be overestimated in those patients, resulting in lower FFR_{CT} value than invasively measured FFR. Third, the whole process takes several hours for the calculation of FFR_{CT} and the accuracy is dependent on the quality of CT images. Advances in technology may solve the problem of long processing time, and lead to broad application.

Transluminal attenuation gradient

Transluminal attenuation gradient (TAG) is a novel process that can assess the severity of coronary stenosis, which is defined as the gradient of intraluminal radiological attenuation. For this analysis, cross-sectional images perpendicular to the vessel centerline were reconstructed for each major coronary artery. The following three variables were measured at 5-mm intervals, from the ostium to the distal portion of the artery where the cross-sectional area fell below 2.0 mm^2: mean diameter (mm), lumen cross-sectional area (mm^2) and luminal radiological attenuation (HU). The vessel centerline as well as the contour of the region of interest were manually corrected, if necessary. Finally, TAG was determined from the change in HU per 10-mm length of the coronary artery, and defined as the linear regression coefficient between luminal radiological attenuation (HU) and length from the ostium (mm). Because TAG is associated not only with the severity of luminal narrowing but also to flow velocity, it can provide information on the functional significance of coronary artery stenosis. Several studies have shown that the value of TAG was correlated well with the degree of diameter stenosis, and could discriminate normal and obstructive coronary arteries [34,35]. Furthermore, addition of TAG significantly improved the diagnostic accuracy of cCTA, especially in coronary arteries with severely calcified lesions [15].

However, TAG also has several limitations (Table 2). Physicians should recognize the confounding factors which can adversely contribute to the results of TAG. For example, TAG may be influenced by various artifacts including imaging smoothing, partial volume effects and beam hardening. More importantly, a recent study revealed that diagnostic performance of TAG was inferior compared with that of FFR_{CT} in vessels with noncalcified or partially calcified plaques (AUC 0.63 vs 0.94, p value <0.001) [16]. Another study showed that TAG could not provide additional diagnostic value over 256-slice cCTA alone in assessing the hemodynamic significance of coronary artery stenosis [36]. This study suggested that the correction of temporal nonuniformity of contrast delivery may improve the diagnostic ability of TAG.

Despite the paucity of data, TAG has particular appeal in so far as this technique has considerable advantages, including no need for additional radiation and lengthy computation. In addition, according to the aforementioned study, the diagnostic performance of TAG was better in vessels with calcified plaques, with no significant difference to that of FFR_{CT} (AUC 0.75 vs 0.92, p value = 0.195) [16]. These findings imply that TAG might be useful in CAD patients with specific conditions causing difficulty in evaluation of coronary arteries, such as severe calcification or restenosis of stent. In addition, considering that the single-beat imaging of whole coronary tress can be ideal for TAG measurement, it is expected that the diagnostic performance of TAG can be further improved with the use of a 320-detector row scanner. Indeed, a quite recent study has shown that TAG using 320-detector row CT plus cCTA can achieve comparable diagnostic accuracy for functional assessment of coronary stenosis to CT-MPI plus cCTA (AUC 0.844 vs 0.845) [37]. This study also suggested that the integration of TAG into CT-MPI and cCTA may provide the better diagnostic accuracy (AUC 0.91) in comparison with TAG plus cCTA or CT-MPI plus cCTA.

The future directions for cCTA-based hemodynamic assessment

Hybrid cardiac imaging

Another way to obtain hemodynamic measurements is the fusion of anatomic and physiologic imaging, so-called hybrid cardiac imaging. Advances in software and hardware make it possible to integrate dual imaging modalities into hybrid system, which can allow combined acquisition of the different data sets. Several studies have investigated the diagnostic performance of this hybrid cardiac imaging, in particular, focusing on the combination of cCTA with conventional myocardial perfusion imaging such as SPECT or positron emission tomography (PET). It has been reported that cardiac hybrid imaging by fusing cCTA with SPECT can provide added diagnostic information for CAD assessment [38]. Furthermore, this cardiac hybrid imaging can aid the decision-making process regarding treatment strategy for CAD [39], and allow risk stratification for adverse clinical events in CAD patients [40]. With regard to the integration of cCTA and PET, evidence has been accumulated to support its feasibility and diagnostic accuracy for CAD assessment [41,42,43,44]. Kajander *et al.* demonstrated that hybrid cardiac imaging with PET/CT can accurately detect CAD in suspected CAD patients, with radiation exposure <10 mSv [42].

Hemodynamic parameters pertaining to plaques

In addition to FFR, the application of CFD technology on cCTA enables noninvasive measurement of other hemodynamic parameters which have important role in the pathogenesis of coronary plaques (Figure 4). For example, wall shear stress (WSS) is a tangential force generated by the friction of blood flow over the vascular endothelial surface. Based on numerous animal and human studies, low WSS has emerged as a key determinant of plaque development and progression [45,46,47], whereas high WSS has been hypothesized to be a potential contributor in plaque destabilization and rupture [48,49,50]. Quite recently, one study has shown that cCTA-based CFD can accurately determine the distribution of WSS in human coronary bifurcation as well as main coronary arteries [51]. In addition to WSS, the CFD simulation in CCTA can be used to measure WSS gradient and time-dependent directional changes in WSS such as oscillatory shear index and relative residence time, which also contribute to plaque progression and vulnerability [52]. These findings have shed light on the potential usefulness of CT-based hemodynamic assessment in predicting plaque behaviors, including plaque development, progression, vulnerability and rupture risk, which goes beyond its traditional role in detecting myocardial ischemia. Moreover, there are experimental attempts to explore the role of other hemodynamic parameters affecting coronary plaques, such as tissue stress and pressure-related forces [53,54,55], which can be assessed by the cCTA-based CFD technology in the future.

Virtual stenting

In addition to the hemodynamic assessment of stenotic lesions as a pretreatment diagnosis, CT-based CFD can also be used to predict the functional outcomes of coronary stenting by the simulation of virtual stenting in a patient-specific coronary artery model (Figure 5).

Virtual stenting is performed by modifying the computational model in the region of the stent to restore the area of the treated coronary segment according to the proximal and distal reference areas. Then, the computational analysis of coronary flow and pressure during hyperemia is repeated to determine post-treatment

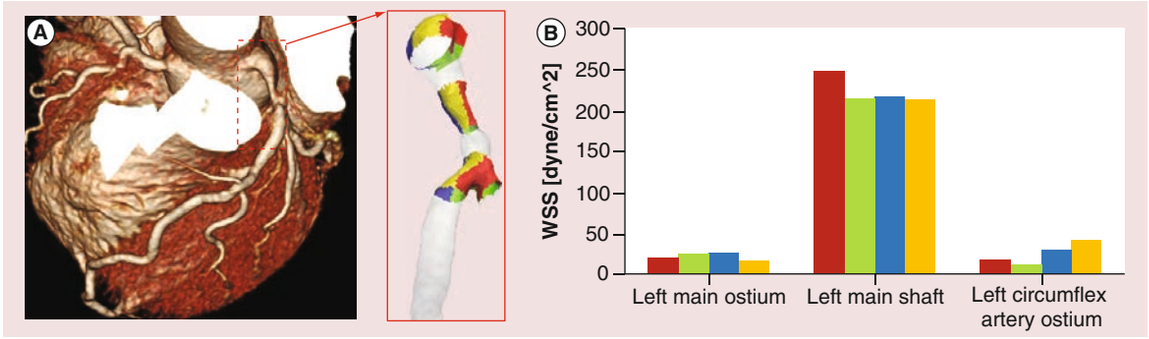

Figure 4. An example of segmental wall shear stress measurement using coronary computed tomography angiography. (A) A color-coded 3D map based on cCTA image demonstrates the distribution of WSS in the left coronary artery. **(B)** The quantification of segmental WSS shows the difference in the magnitude and distribution of WSS according to the portion of the left main coronary artery.
cCTA: Coronary computed tomography angiography; WSS: Wall shear stress.

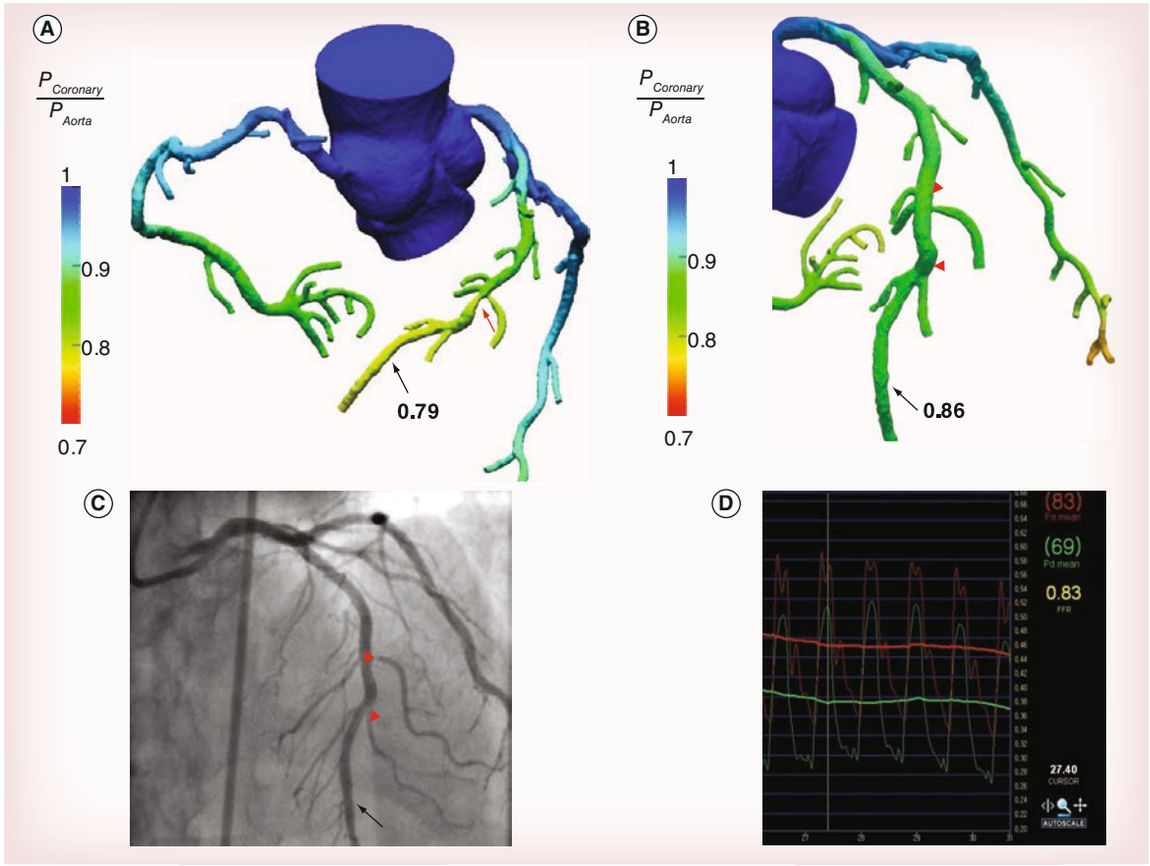

Figure 5. A representative case of virtual stenting. (A) A focal stenosis (red arrow) causing ischemia (black arrow) is demonstrated in LAD, which is the case shown in Figure 3.
(B) After virtual stenting (red arrow heads), FFR_{CT} demonstrates no residual significant ischemia in LAD, with a computed value of 0.86 (black arrow).
(C–D) After successful stent implantation to distal LAD stenosis (red arrow heads), invasive FFR is 0.83 (black arrow), confirming the simulation results of FFR_{CT}.
FFR: Fractional flow reserve; FFR_{CT}: Computed tomography-derived fractional flow reserve; LAD: Left anterior descending coronary artery.

FFR_{CT}. In a pilot study, when compared with invasive FFR, the diagnostic accuracy of FFR_{CT} to predict the residual ischemia after stenting was 96%, with sensitivity of 100% and specificity of 96% [56]. Although the available data are limited, this technology of virtual stenting can be especially useful for guiding the revascularization strategy in patients with complex CAD. In patients with serial stenotic lesions, it is difficult to discriminate the hemodynamic significance of each lesion, even using invasive FFR, unless the other stenoses are treated. Virtual stenting and FFR_{CT}, however, can make it possible to precisely measure the hemodynamic significance of each stenotic lesion. Hence, this novel technology can tailor the treatment plan based on the simulation results, which may lead to the reduction of unnecessary interventions, procedure time, costs and radiation exposure. In theory, FFR_{CT} is also applicable to predict the functional outcomes after coronary artery bypass graft surgery. Future studies exploring these concepts can pave the way for the CT-based noninvasive 'all-in-one' diagnostic and treatment approach.

Conclusion

Noninvasive hemodynamic assessment using cCTA is feasible and helpful in the detection of myocardial ischemia in CAD patients. Presently, CT-MPI, FFR_{CT} and TAG represent significant advances in this field, and each technique can provide valuable information on the identification of ischemia, with its own strength and limitation. Further studies enable widespread clinical adaptation of these promising technologies. Furthermore, in the future, the application of cCTA-based hemodynamic assessment can be extended to the treatment planning and future risk estimation for the patients with CAD, beyond the detection of myocardial ischemia.

Future perspective

The evolution of CT technology can allow more sophisticated morphometric analysis of coronary plaques as well as better determination of the degree of stenosis. In this regard, coupling advanced hemodynamic assessment with more reliable morphological data have improved the diagnostic accuracy of noninvasive detection of flow-limiting stenosis and myocardial ischemia. In the future, further advances in CT technology will lead to a comprehensive assessment of anatomic and physiologic metrics of coronary atherosclerotic plaques and thus provide convincing opportunities for the noninvasive risk assessment for future cardiovascular events. This CT-based risk assessment can also be combined with metabolic information of plaques by using hybrid scanners and novel contrast agents. Furthermore, the integration of bioinformatics analysis of various 'omics' data with CT-based plaque assessment can further aid the identification of patients with subclinical CAD and vulnerable plaques.

Acknowledgement

The authors thank DH Yang from Asan Medical Center for his support in writing this article.

Financial & competing interests disclosure

The authors have no relevant affiliations or financial involvement with any organization or entity with a financial interest in or financial conflict with the subject matter or materials discussed in the manuscript. This includes employment, consultancies, honoraria, stock ownership or options, expert testimony, grants or patents received or pending or royalties.

No writing assistance was utilized in the production of this manuscript.

Executive summary

- Modern computed tomography technology has enabled noninvasive hemodynamic assessment in patients with coronary artery disease.
- Computed tomography (CT)-myocardial perfusion imaging is proposed as a relatively easy-to-perform tool to detect myocardial ischemia with an advantage of direct visualization of myocardial perfusion.
- CT-derived fractional flow reserve is a technique based on computational fluid dynamics, which can define the stenotic lesion causing myocardial ischemia, with no requirement of additional medication or radiation exposure.
- Transluminal attenuation gradient by CT is another promising way to identify the flow-limiting stenosis, although fewer data exist to support the diagnostic performance of transluminal attenuation gradient than that of CT-myocardial perfusion imaging and CT-derived fractional flow reserve.
- CT-based hemodynamic assessment can be combined with other imaging modalities (e.g., hybrid cardiac imaging) in the hope of an improved diagnostic performance to detect myocardial ischemia. Its application can be extended beyond the detection of ischemia such as noninvasive assessment of other hemodynamic forces affecting plaques and computational fluid dynamics-based simulation of treatment plans.

References

1 Pijls NH, De Bruyne B, Peels K *et al.* Measurement of fractional flow reserve to assess the functional severity of coronary-artery stenoses. *N. Engl. J. Med.* 334(26), 1703–1708 (1996).

2 Tonino PA, De Bruyne B, Pijls NH *et al.* Fractional flow reserve versus angiography for guiding percutaneous coronary intervention. *N. Engl. J. Med.* 360(3), 213–224 (2009).

3 De Bruyne B, Pijls NH, Kalesan B *et al.* Fractional flow reserve-guided PCI versus medical therapy in stable coronary disease. *N. Engl. J. Med.* 367(11), 991–1001 (2012).

4 Kern MJ, Lerman A, Bech JW *et al.* Physiological assessment of coronary artery disease in the cardiac catheterization laboratory: a scientific statement from the American Heart Association Committee on Diagnostic and Interventional Cardiac Catheterization, Council on Clinical Cardiology. *Circulation* 114(12), 1321–1341 (2006).

5 Task Force on Myocardial Revascularization of the European Society Of C, The European Association for Cardio-Thoracic S, European Association for Percutaneous Cardiovascular I *et al.* Guidelines on myocardial revascularization. *Eur. Heart J.* 31(20), 2501–2555 (2010).

6 Patel MR, Dehmer GJ, Hirshfeld JW, Smith PK, Spertus JA. ACCF/SCAI/STS/AATS/AHA/ASNC/HFSA/SCCT 2012 Appropriate use criteria for coronary revascularization focused update: a report of the American College of Cardiology Foundation Appropriate Use Criteria Task Force, Society for Cardiovascular Angiography and Interventions, Society of Thoracic Surgeons, American Association for Thoracic Surgery, American Heart Association, American Society of Nuclear Cardiology, and the Society of Cardiovascular Computed Tomography. *J. Am. Coll. Cardiol.* 59(9), 857–881 (2012).

7 Kim HJ, Vignon-Clementel IE, Coogan JS, Figueroa CA, Jansen KE, Taylor CA. Patient-specific modeling of blood flow and pressure in human coronary arteries. *Ann. Biomed. Eng.* 38(10), 3195–3209 (2010).

8 Taylor CA, Fonte TA, Min JK. Computational fluid dynamics applied to cardiac computed tomography for noninvasive quantification of fractional flow reserve: scientific basis. *J. Am. Coll. Cardiol.* 61(22), 2233–2241 (2013).

9 Koo BK, Erglis A, Doh JH *et al.* Diagnosis of ischemia-causing coronary stenoses by noninvasive fractional flow reserve computed from coronary computed tomographic angiograms. Results from the prospective multicenter DISCOVER-FLOW (Diagnosis of Ischemia-Causing Stenoses Obtained Via Noninvasive Fractional Flow Reserve) study. *J. Am. Coll. Cardiol.* 58(19), 1989–1997 (2011).

10 Min JK, Leipsic J, Pencina MJ *et al.* Diagnostic accuracy of fractional flow reserve from anatomic CT angiography. *JAMA* 308(12), 1237–1245 (2012).

11 Norgaard BL, Leipsic J, Gaur S *et al.* Diagnostic performance of noninvasive fractional flow reserve derived from coronary computed tomography angiography in suspected coronary artery disease: the NXT trial (Analysis of Coronary Blood Flow Using CT Angiography: Next Steps). *J. Am. Coll. Cardiol.* 63(12), 1145–1155 (2014).

12 Blankstein R, Shturman LD, Rogers IS *et al.* Adenosine-induced stress myocardial perfusion imaging using dual-source cardiac computed tomography. *J. Am. Coll. Cardiol.* 54(12), 1072–1084 (2009).

13 George RT, Arbab-Zadeh A, Miller JM *et al.* Adenosine stress 64- and 256-row detector computed tomography angiography and perfusion imaging: a pilot study evaluating the transmural extent of perfusion abnormalities to predict atherosclerosis causing myocardial ischemia. *Circ. Cardiovasc. Imaging* 2(3), 174–182 (2009).

14 Ho KT, Chua KC, Klotz E, Panknin C. Stress and rest dynamic myocardial perfusion imaging by evaluation of complete time-attenuation curves with dual-source CT. *JACC Cardiovasc. Imaging* 3(8), 811–820 (2010).

15 Choi JH, Min JK, Labounty TM *et al.* Intracoronary transluminal attenuation gradient in coronary CT angiography for determining coronary artery stenosis. *JACC Cardiovasc. Imaging* 4(11), 1149–1157 (2011).

16 Yoon YE, Choi JH, Kim JH *et al.* Noninvasive diagnosis of ischemia-causing coronary stenosis using CT angiography: diagnostic value of transluminal attenuation gradient and fractional flow reserve computed from coronary CT angiography compared with invasively measured fractional flow reserve. *JACC Cardiovasc. Imaging* 5(11), 1088–1096 (2012).

17 Techasith T, Cury RC. Stress myocardial CT perfusion: an update and future perspective. *JACC Cardiovasc. Imaging* 4(8), 905–916 (2011).

18 George RT, Silva C, Cordeiro MA *et al.* Multidetector computed tomography myocardial perfusion imaging during adenosine stress. *J. Am. Coll. Cardiol.* 48(1), 153–160 (2006).

19 Kurata A, Mochizuki T, Koyama Y *et al.* Myocardial perfusion imaging using adenosine triphosphate stress multi-slice spiral computed tomography: alternative to stress myocardial perfusion scintigraphy. *Circ. J.* 69(5), 550–557 (2005).

20 Ko BS, Cameron JD, Leung M *et al.* Combined CT coronary angiography and stress myocardial perfusion imaging for hemodynamically significant stenoses in patients with suspected coronary artery disease: a comparison with fractional flow reserve. *JACC Cardiovasc. Imaging* 5(11), 1097–1111 (2012).

21 Feuchtner G, Goetti R, Plass A *et al.* Adenosine stress high-pitch 128-slice dual-source myocardial computed tomography perfusion for imaging of reversible myocardial ischemia: comparison with magnetic resonance imaging. *Circ. Cardiovasc. Imaging* 4(5), 540–549 (2011).

22 Bamberg F, Klotz E, Flohr T *et al.* Dynamic myocardial stress perfusion imaging using fast dual-source CT with alternating table positions: initial experience. *Eur. Radiol.* 20(5), 1168–1173 (2010).

23 Rossi A, Uitterdijk A, Dijkshoorn M *et al.* Quantification of myocardial blood flow by adenosine-stress CT perfusion imaging in pigs during various degrees of stenosis correlates well with coronary artery blood flow and fractional flow reserve. *Eur. Heart J. Cardiovasc. Imaging* 14(4), 331–338 (2013).

24 Gramer BM, Muenzel D, Leber V *et al.* Impact of iterative reconstruction on CNR and SNR in dynamic myocardial perfusion imaging in an animal model. *Eur. Radiol.* 22(12), 2654–2661 (2012).

25 Al Jaroudi W, Iskandrian AE. Regadenoson: a new myocardial stress agent. *J. Am. Coll. Cardiol.* 54(13), 1123–1130 (2009).

26 Iqbal FM, Hage FG, Ahmed A *et al.* Comparison of the prognostic value of normal regadenoson with normal adenosine myocardial perfusion imaging with propensity score matching. *JACC Cardiovasc. Imaging* 5(10), 1014–1021 (2012).

27 Williams MC, Newby DE. CT myocardial perfusion: a step towards quantification. *Heart* 98(7), 521–522 (2012).

28 Hecht HS. The game changer? *J. Am. Coll. Cardiol.* 63(12), 1156–1158 (2014).

29 Einstein AJ. TAG-is it it?: improving coronary computed tomography angiography with the isotemporal transluminal contrast attenuation gradient. *J. Am. Coll. Cardiol.* 61(12), 1280–1282 (2013).

30 Fihn SD, Gardin JM, Abrams J *et al.* 2012 ACCF/AHA/ACP/AATS/PCNA/SCAI/STS Guideline for the diagnosis and management of patients with stable ischemic heart disease: a report of the American College of Cardiology Foundation/American Heart Association Task Force on Practice Guidelines, and the American College of Physicians, American Association for Thoracic Surgery, Preventive Cardiovascular Nurses Association, Society for Cardiovascular Angiography and Interventions, and Society of Thoracic Surgeons. *J. Am. Coll. Cardiol.* 60(24), e44–e164 (2012).

31 Leng X, Scalzo F, Ip HL *et al.* Computational fluid dynamics modeling of symptomatic intracranial atherosclerosis may predict risk of stroke recurrence. *PLoS ONE* 9(5), e97531 (2014).

32 Karmonik C, Partovi S, Loebe M *et al.* Computational fluid dynamics in patients with continuous-flow left ventricular assist device support show hemodynamic alterations in the ascending aorta. *J. Thorac. Cardiovasc. Surg.* 147(4), 1326–1333 e1321 (2014).

33 Nieman K, De Feijter PJ. Aerodynamics in Cardiac CT. *Circ. Cardiovasc. Imaging* 6(6), 853–854 (2013).

34 Steigner ML, Mitsouras D, Whitmore AG *et al.* Iodinated contrast opacification gradients in normal coronary arteries imaged with prospectively ECG-gated single heart beat 320-detector row computed tomography. *Circ. Cardiovasc. Imaging* 3(2), 179–186 (2010).

35 Lackner K, Bovenschulte H, Stutzer H, Just T, Al-Hassani H, Krug B. In vitro measurements of flow using multislice computed tomography (MSCT). *Int. J. Cardiovasc. Imaging* 27(6), 795–804 (2011).

36 Stuijfzand WJ, Danad I, Raijmakers PG *et al.* Additional value of transluminal attenuation gradient in CT angiography to predict hemodynamic significance of coronary artery stenosis. *JACC Cardiovasc. Imaging* 7(4), 374–386 (2014).

37 Wong DT, Ko BS, Cameron JD *et al.* Comparison of diagnostic accuracy of combined assessment using adenosine stress computed tomography perfusion + computed tomography angiography with transluminal attenuation gradient + computed tomography angiography against invasive fractional flow reserve. *J. Am. Coll. Cardiol.* 63(18), 1904–1912 (2014).

38 Sato A, Nozato T, Hikita H *et al.* Incremental value of combining 64-slice computed tomography angiography with stress nuclear myocardial perfusion imaging to improve noninvasive detection of coronary artery disease. *J. Nucl. Cardiol.* 17(1), 19–26 (2010).

39 Pazhenkottil AP, Nkoulou RN, Ghadri JR *et al.* Impact of cardiac hybrid single-photon emission computed tomography/computed tomography imaging on choice of treatment strategy in coronary artery disease. *Eur. Heart J.* 32(22), 2824–2829 (2011).

40 Pazhenkottil AP, Nkoulou RN, Ghadri JR *et al.* Prognostic value of cardiac hybrid imaging integrating single-photon emission computed tomography with coronary computed tomography angiography. *Eur. Heart J.* 32(12), 1465–1471 (2011).

41 Namdar M, Hany TF, Koepfli P *et al.* Integrated PET/CT for the assessment of coronary artery disease: a feasibility study. *J. Nucl. Med.* 46(6), 930–935 (2005).

42 Kajander S, Joutsiniemi E, Saraste M *et al.* Cardiac positron emission tomography/computed tomography imaging accurately detects anatomically and functionally significant coronary artery disease. *Circulation* 122(6), 603–613 (2010).

43 Di Carli MF, Dorbala S, Meserve J, El Fakhri G, Sitek A, Moore SC. Clinical myocardial perfusion PET/CT. *J. Nucl. Med.* 48(5), 783–793 (2007).

44 Sampson UK, Dorbala S, Limaye A, Kwong R, Di Carli MF. Diagnostic accuracy of rubidium-82 myocardial perfusion imaging with hybrid positron emission tomography/computed tomography in the detection of coronary artery disease. *J. Am. Coll. Cardiol.* 49(10), 1052–1058 (2007).

45 Samady H, Eshtehardi P, Mcdaniel MC *et al.* Coronary artery wall shear stress is associated with progression and transformation of atherosclerotic plaque and arterial remodeling in patients with coronary artery disease. *Circulation* 124(7), 779–788 (2011).

46 Stone PH, Saito S, Takahashi S *et al.* Prediction of progression of coronary artery disease and clinical outcomes using vascular profiling of endothelial shear stress and arterial plaque characteristics: the PREDICTION Study. *Circulation* 126(2), 172–181 (2012).

47 Gambillara V, Chambaz C, Montorzi G, Roy S, Stergiopulos N, Silacci P. Plaque-prone hemodynamics impair endothelial function in pig carotid arteries. *Am. J. Physiol. Heart Circ. Physiol.* 290(6), H2320–H2328 (2006).

48 Dolan JM, Kolega J, Meng H. High wall shear stress and spatial gradients in vascular pathology: a review. *Ann. Biomed. Eng.* 41(7), 1411–1427 (2013).

49 Slager CJ, Wentzel JJ, Gijsen FJ *et al.* The role of shear stress in the destabilization of vulnerable plaques and related therapeutic implications. *Nat. Clin. Pract. Cardiovasc. Med.* 2(9), 456–464 (2005).

50 Slager CJ, Wentzel JJ, Gijsen FJ *et al.* The role of shear stress in the generation of rupture-prone vulnerable plaques. *Nat. Clin. Pract. Cardiovasc. Med.* 2(8), 401–407 (2005).

51 Gijsen FJ, Schuurbiers JC, Van De Giessen AG, Schaap M, Van Der Steen AF, Wentzel JJ. 3D reconstruction techniques of human coronary bifurcations for shear stress computations. *J. Biomech.* 47(1), 39–43 (2014).

52 Rikhtegar F, Knight JA, Olgac U *et al.* Choosing the optimal wall shear parameter for the prediction of plaque location-A patient-specific computational study in human left coronary arteries. *Atherosclerosis* 221(2), 432–437 (2012).

53 Asanuma T, Higashikuni Y, Yamashita H, Nagai R, Hisada T, Sugiura S. Discordance of the areas of peak wall shear stress and tissue stress in coronary artery plaques as revealed by fluid-structure interaction finite element analysis: a case study. *Int. Heart J.* 54(1), 54–58 (2013).

54 Li ZY, Taviani V, Gillard JH. The impact of wall shear stress and pressure drop on the stability of the atherosclerotic plaque. *Conf. Proc. IEEE Eng. Med. Biol. Soc.* 1373–1376 (2008).

55 Li ZY, Taviani V, Tang T *et al.* The mechanical triggers of plaque rupture: shear stress vs pressure gradient. *Br. J. Radiol.* 82, S39–S45 (2009).

56 Kim KH, Doh JH, Koo BK *et al.* A novel noninvasive technology for treatment planning using virtual coronary stenting and computed tomography-derived computed fractional flow reserve. *JACC Cardiovasc. Interv.* 7(1), 72–78 (2014).